Paper No.
03057

CORROSION 2003

EIS INVESTIGATIONS OF ALKYD AND EPOXY COATINGS AS THEY ARE CHEMICALLY STRIPPED FROM STEEL PANELS

Mike O'Donoghue, Ph.D., Ron Garrett and V.J. Datta
ICI Devoe Coatings Company
1609 Boundary Road
Vancouver, BC V5K 4X7

Terry J. Aben, M.A.Sc., P.Eng
Powertech Labs. Inc.
12388-88th Avenue
Surrey, BC V3W 7R7

Clive Hare
Coating System Design Inc.
PO Box 859, 21 Pickens Street
Lakeville, MA 02347

ABSTRACT

Electrochemical Impedance Spectroscopy (EIS) has been employed to monitor, and model, real-time chemical stripping and de-adhesion of select coatings from steel panels. Instead of the customary salt solution, a water based chemical stripper was used in a custom-built EIS cell. In effect, the stripper was simultaneously used as the electrolyte for the EIS test as well as the modus operandi for stripping the coated panels.

Alkyd (3 coats) and epoxy polyamide coatings (2 coats) were compared and contrasted during the chemical stripping process. To examine the influence of pigment types in the coatings, a leafing aluminum alkyd finish in a 3 coat system was compared with an alkyd finish that contained titanium dioxide. The epoxy polyamide coating systems examined contained either non-leafing aluminum or titanium dioxide pigments.

The EIS data is discussed in terms of such multivariate factors as the pigment used in the different coating types, the influence of coating chemistry and the unique chemistry of the water based chemical stripper.

Keywords: alkyd, epoxy, aluminum pigments, titanium dioxide pigments, electrochemical impedance spectroscopy, EIS, chemical strippers, SARA

Copyright
©2003 by NACE International. Requests for permission to publish this manuscript in any form, in part or in whole must be in writing to NACE International, Publications Division, 1440 South Creek Drive, Houston, Texas 77084-4906. The material presented and the views expressed in this paper are solely those of the author(s) and not necessarily endorsed by the Association. Printed in U.S.A.

INTRODUCTION

In an age of far reaching regulatory imposition, environmentally friendly and water based chemical strippers have increasingly enjoyed favor as a surface preparation alternative for industrial and marine refurbishment projects. While abrasive blasting is used extensively, and generally continues to be the preferred method of surface preparation, increasingly there are many instances where for environmental or economic reasons it is prohibited, impractical or impossible to carry out. Under these circumstances the use of chemical strippers often becomes an attractive and cost-effective surface preparation alternative.

A new class of chemical strippers, described by the acronym SARA (Selective Adhesion Release Agents), have recently been reported to possess a broader spectrum stripping efficacy than either bond breakers and caustics (1-3). Of considerable interest to the authors was the fact that SARA chemical strippers are water-based macro-emulsions (where the dispersed droplet particle size is from about 0.2 to about 50 microns) and therefore conducive to use in EIS test cells for real-time stripping investigation using this technique.

By harnessing the versatility of SARA water-based chemical strippers in conjunction with the diagnostic ability of EIS, a unique and accelerated test method was developed to shed new light upon the barrier properties of coatings. In particular, the benefit of using different types of pigments in coatings could begin to be scrutinized in a fresh way so as ultimately to enhance future coatings development.

CANDIDATE MATERIALS

1. Rationale for chemical stripper selection

A fundamental requirement in the present work was to obtain a water based chemical stripper that could be used in an EIS cell in lieu of the customary salt solution. The SARA chemical stripper selected met this requirement. Furthermore, it was known to effectively strip numerous thermoplastic and thermoset coatings according to the following mechanism reported by one of the authors (MOD) in a previous publication (1).

Phase 1: Progressively softening and stressing the coating to be stripped, the SARA chemical stripper penetrates free volume holes in the coating film as it diffuses to the substrate. While this occurs, a paraffinic phase in the stripper migrates to the superficial surface of the stripper and in so doing increases the residence time of the stripper in the coating film. These are essentially the three elements of penetrant diffusion, penetrant solubility and wax precipitation that are manifested by methylene chloride and NMP/DBE based strippers (2).

Phase 2 : The SARA stripper has at this point essentially penetrated the entire film and closes on the metallic interface. Under a dramatic destabilization of the coating's bond to the metal from compressive swelling and deformation of the film, a negative pressure P1 develops along the interface. In addition, the degradation of a proprietary ingredient of the SARA remover is catalyzed by the metal substrate itself. This will, in Phase 3, add uniquely to the stripping action.

Phases 1 and 2 summarize the mechanisms of the diffusion - coating stressing step.

Phase 3 : As soon as the SARA stripper has accessed the metallic substrate, the catalytic degradation of the proprietary ingredient by the metal results in the evolution of nascent oxygen. This immediately combines to form molecular oxygen, which sets up a positive pressure, P2 at the interface. A pressure inversion then occurs due to the pressure differential between P2 and P1.

This sudden pressure transition/equilibration at the interface intensifies de-adhesion (lateral and vertical coating detachment) and is sometimes accompanied by actual audible popping or snapping sounds. Thus the coating de-adhesion step is initiated.

Continued swelling of the film and continued production of oxygen propagate the stripping action, and adhesive sites across the interface are continuously disrupted. Termination of the latter propagation of de-adhesion occurs only when the film is essentially free from the substrate, when the compressive stresses within the film are essentially fully dissipated. (It should be noted that frequently isolated bonds may remain intact across the interface).

2. Rationale for alkyd and epoxy coatings selection

2 (a) Alkyd

Alkyds are a class of oil modified polyesters that are synthesized by the reaction of polyhydric alcohols with polybasic acids. For many years alkyds have been the most widely used of the synthetic resins and aluminum filled alkyd barrier finishes have been used on a variety of steel surfaces where extra barrier protection was deemed necessary. Ideally, in these systems, leafing aluminum pigments (bearing low surface energy stearic acid treatments) are not readily wetted by the binder phase of the coating. The pigments, therefore, tend to be drawn to the surface of the film under surface tension. Here they pack, orientating themselves laterally to the substrate, and presenting an enhanced metallic barrier to would be penetrants. If wiped with a dry cloth these films will often release unbound aluminum flake onto the cloth. The extra barrier properties afforded by flake, leafing aluminum pigments arises from their platelet overlap to provide a more tortuous path for moisture or other penetrants to reach the steel-polymer interface (4,5).

Unfortunately many low surface energy chemical species tend to reduce the leafing efficiency of the stearic acid coated aluminum flakes. They do this by either stripping the coating from the pigments (acidic binders, heat and excessive mechanical dispersion) or by lowering the surface energy of the binder below that of the pigment. These low surface energy "deleafers" include most surfactants and surfactant like moieties (lead and calcium driers) and many high wetting solvents (not only polar solvents such as alcohols but even low energy non-polar solvents such as V.M. & P. Naphtha). All of these materials tend to improve the wetting of the pigment by the wet binder. Well-wetted aluminum flake does not tend to float out of the wet film and stratify at its surface, but is well distributed throughout the film thickness. Leafing will also be greatly impeded in highly viscous films. In an age of low VOC system this may be singularly problematic.

Partially "deleafed" films, like these, are generally less metallic in appearance, being less silvery and more gray than are fully leafed films. Unlike the fully leafed films, such films will not release aluminum when wiped with a dry cloth.

The authors wanted to investigate this platelet effect of the aluminum and compare, at least at a rudimentary level, the alkyd's susceptibility to de-adhesion from steel as a function of aluminum (barrier) or titanium dioxide (opacity) pigments. Given that alkyds possess only a fair resistance to solvents they were expected to be stripped from steel panels in a fairly short period of time as EIS experiments were undertaken. In this way, alkyds were envisioned to be good vehicles to quickly differentiate the overall effect of either leafing aluminum or titanium dioxide pigments in their formulations.

The alkyd resin of the primer was chain stopped with benzylic acid and based on a tall oil fatty acid. It had an oil length of 60 % and an acid value between 10 and 12 mg KOH/g of alkyd. In

contrast, the alkyd resins (blend of long oil and medium oil) used in the intermediate and topcoats was based on soya oils. It had an oil length of 57% (medium) and 60% (long) and an acid value of 10 mg KOH/g of alkyd.

2 (b) Epoxy polyamide

In epoxy systems aluminum pigments do not leaf as they do in alkyds. Ingredients such as alcohols, glycol ethers, ketones, and other polar components such as curing agents (amines as well as polyamides) tend to de-leaf the aluminum (dissolve, react with or otherwise strip, the fatty acid treatment from the pigment). This renders the pigment more easily wet by the binder. The improved wetting eliminates any tendency of the pigment to stratify at the surface and results in less lateral heterogeneity. The aluminum platelets are more randomly distributed throughout the coating thickness, and lie at all levels of the film, presumably well separated by resinous binder.

In the context of chemical stripping, it was known from previous work that amine-cured epoxies would provide superior solvent resistance compared to polyamide epoxies and fully functional novolac epoxies could not be chemically stripped in a reasonable time frame. Importantly, what the authors needed in the present work was an epoxy aluminum mastic and titanium dioxide pigmented epoxy that could be successfully stripped in a time frame suited to tracking by EIS. A traditional surface tolerant epoxy polyamide met these criteria. Furthermore, with other things being equal in terms of titanium dioxide pigment selection, it was reasoned that the epoxy would provide a stark contrast to the alkyd vis a vis resin resistance during the chemical stripping process. Furthermore, it promised to be interesting to compare the effect of the de-leafed aluminum in the epoxy coating versus the leafing aluminum in the alkyd coating system.

EXPERIMENTAL AND TEST PROCEDURES

1. Aged Panel Preparation

Hot rolled steel test panels (ca. 16 gauge) measuring 4 by 6 inches (10 by 12.25 cm) were abrasive blasted to produce an SSPC-SP10 Near White Metal Standard and a jagged 1.5-2.5 mil profile.

2. Systems Tested and Coating Application

Two coats of epoxy polyamide were spray applied in the laboratory at ca. 5 mils DFT per coat using conventional spray equipment (77°F and 55% relative humidity). The coated steel panels were allowed to age approximately two years prior to conducting chemical stripping experiments.

A three coat alkyd system containing titanium dioxide pigmentation in each coat consisted of 2 coats of primer (ca. 2 mils DFT/coat) and a medium oil finish coat (ca. 2 mils DFT). For contrast, another three coat alkyd system was selected where the primer and mid coats were the same and the finish coat was a medium oil alkyd containing leafing aluminum. Both alkyd systems were spray applied in a fabricators shop using conventional spray equipment (ca. 70°F and 75% relative humidity). After curing at ambient conditions for fourteen days, the coated steel test panels were then subjected to 1000 hours accelerated weathering exposure in an ultraviolet-condensing (UV-CON) chamber according to ASTM G53. This was necessary to age the alkyd coating system and reasonably simulate its long term exposure to field conditions.

3. SEM and Optical Microscopy

Steel samples for the microscopy were prepared by cutting the steel samples with a fine bandsaw, potting in epoxy pigmented with silica fume, and polishing. The SEM instrument used in the work was a Hitachi S2500. All images were Back scattered Electron Images (BEI) and produced at 25kV accelerating voltage with high resolution digital imaging and editing processes.

Optical micrographs of the steel substrate-stripped coating interface were taken at 50 times magnification using a Leica MZ12 stereoscopic microscope.

4. Electrochemical Impedance Spectroscopy (EIS)

4.1 The technique

Electrochemical Impedance Spectroscopy (EIS) has been proven to be a powerful technique for rapidly, quantitatively and non-destructively evaluating the performance of coated metals. EIS allows the quantitative determination of several coating properties without affecting the coating and its performance, and detection of changes in a coating's behavior at a small fraction of the exposure time required for those changes to be detectable by the traditional mechanical or visual inspection methods.

Organic coatings act as barriers between the metal substrate and the environment, reducing the rate at which water, oxygen, and corrosion inducing agents (such as depassivating ions) reach the metal surface, thereby delaying and preventing corrosion. The barrier properties of organic coatings also create a high electrical resistance across the coating thickness (6). As coatings age in a corrosive environment, the interconnecting network of pores within the coating eventually become saturated with water, salts, etc., exposing the metal substrate to a corrosive environment. The saturation of the pores also creates paths of lower electrical resistance through the coating.

Aged organic coating systems also possess other electrical properties. The coating materials have dielectric properties, which cause them to act as capacitors to an electrical current. Corrosion occurring at a metal surface has a polarization resistance related to the corrosion rate, and an electric double layer that also behaves as a capacitor. The capacitive properties cannot be identified and separated from the resistive or barrier properties by making a simple resistive measurement.

An EIS measurement consists of attaching a glass cell containing a counter electrode, a reference electrode, and a conductive solution to the coated metal panel. A small sinusoidal AC current signal is applied between the counter electrode and the sample substrate while the resulting voltage response is monitored between the reference electrode and the sample substrate. The AC signal measurement is performed at several frequencies between 100 kHz and 0.1 Hz. From the results obtained the electrical impedance and phase shift of the coated sample are determined as a function of frequency. In essence, impedance in AC electronics is analogous to resistance in DC electronics.

By analyzing the impedance and phase shift vs. frequency plot, several characteristics of the coating under investigation can be determined. In the corrosion and coatings technical literature, it has become widely held that coatings with an impedance over $10^8 \Omega cm^2$ at 0.1Hz are considered

to provide excellent corrosion protection, while those possessing less than $10^6 \Omega cm^2$ are considered to provide poor corrosion protection (7).

4.2 Experimental

Figure T1 shows the EIS test assembly used in the present work. The electrochemical cell used for EIS measurements was a modified version of the Gamry PTC1 Paint Test Cell, which is specifically designed for use with coated metal panels. This cell consists of a tube shaped glass cell that is clamped and sealed to the sample panel with a rubber O-ring, which is filled with the test electrolyte. The PTC1 cell contains a saturated calomel reference electrode and an activated graphite rod counter electrode, both of which are inserted through the top of the cell via a rubber bung.

In normal use, the test electrolyte is a simple aqueous salt solution. This allows the calomel reference electrode to be inserted directly into the test electrolyte without risk of contaminating the reference electrode, as the salt migration into the reference electrode from the test electrolyte is negligible.

For the present study, however, in order to monitor the effect of the SARA stripper on the coating in real time, the EIS measurements had to be made using the stripping solution as the test electrolyte. As the SARA stripper contained components to aid and enhance its diffusion through microporous networks in coatings, the reference electrode could not be inserted directly into the stripper itself. Also, diffusion of salt from the reference electrode into the SARA stripper would have deleterious effects on the stripper's effectiveness. Therefore a custom Luggin capillary was fabricated to separate the reference electrode from the SARA stripper solution without affecting the EIS measurements.

The custom Luggin capillary consisted of a glass tube that was (a) narrow at the lower end and terminating in an extra-fine porous glass plug and (b) wide enough at the top end to allow insertion of the calomel electrode. The tube was filled with a saturated KCl solution, and the reference electrode inserted into the top end through a rubber bung which sealed the end.

Once the Luggin capillary and reference electrode was assembled, the assembly was allowed to rest for approximately an hour to allow the pressure across the porous plug to equilibrate. When the pressure equilibrium was established the rubber bung seal effectively produced a vacuum lock in the capillary, preventing any fluid flow across the porous plug. This, in combination with the microporosity of the porous plug, eliminated the diffusion of salt into the stripping solution. Additionally, the diffusion of the stripping solution into the Luggin capillary was minimized, where it would be greatly diluted before reaching the reference electrode. The saturated KCl solution was highly conductive and eliminated any IR drop in the capillary which would otherwise affect the EIS measurements.

The electronic equipment used to conduct EIS measurements were Gamry PC4/300 Potentiostat / Frequency Response Analyzer boards that had been installed into a PC. A Gamry EIS300 control software package was used to control the test operation, record test data, and create a custom script for experimental control (from its special scripting language). Importantly, a script was developed to perform repeated EIS measurements at preset intervals. The latter facilitated

automated and continuous EIS evaluations throughout the stripping process for each coating tested.

Electrochemical responses of each coating type during chemical stripping were evaluated by attaching and clamping the PTC1 cell to the coated panel, filling the cell with the SARA stripper, inserting the test electrodes, and immediately initiating the programmed test script of EIS evaluations. The test script carried out EIS measurements until the test operator determined from the latest EIS scan that the coating was fully stripped whereupon the test was terminated. The parameters for each EIS measurement were as follows:

Test Area:	14.6 cm^2
Frequency Range:	100 kHz to 0.1 Hz
# of Data Points:	5 points per decade of frequency
Induced DC Potential:	-0.7 V_{SCE}
Induced AC Potential:	+/- 0.01V

During the initial stages of each coating's exposure, the free corrosion potential of the steel substrate could not be detected. Therefore, a DC potential roughly correlating to the free corrosion potential of steel in a non-corrosive neutral pH environment was induced to prevent the potentiostat from inducing potentials that could be detrimental to the samples and itself.

The Gamry EIS300 software also included a collection of programmed macros for MS Excel to provide detailed data analysis of the EIS measurement results. For instance, the macros included tools to fit EIS test results to equivalent circuit models. In this way the fitted values of each circuit element in the model could be quantitatively determined. The circuit model used in the present study is shown in Figure T2. It is based on the known physical and electrical properties of coatings and electrochemical corrosion behavior. The relationship between the circuit elements in the model and the coating and corrosion properties is presented in Figure 3.

The circuit model employed in this work has been commonly used in other publications for EIS coatings studies, albeit with one modification. The aqueous salt electrolytes normally used do not have a capacitive property and thus the circuit models do not include a solution capacitance. However, the organic components contained within the SARA stripper macroemulsion were found to possess dielectric properties. Hence, a solution capacitance was incorporated into the circuit model in this study.

After the chemical stripping – EIS tests were completed for each candidate coating system, the circuit model was fit to the data from each individual EIS scan, and the values for each circuit element determined. An example of the circuit model fit of the data from an individual EIS scan is presented in Figure 4.

RESULTS AND DISCUSSION

Epoxy Polyamide Coating with Titanium Dioxide Pigment

Figures 5 and 6 show the impedance and phase angle results for the epoxy polyamide coating (with titanium dioxide pigment) at several stages throughout the stripping process. These figures reveal interesting trends in the impedance and phase angle behavior as a function of time, all of which illustrate the progressively increasing effect of the SARA stripper on the coating during the stripping process.

Figure 7 is a graph of the impedance at 0.1 Hz vs. exposure time, the most commonly used EIS parameter for evaluating the quality of a protective coating (8). Figures 8 and 9 show the values of the fitted circuit model elements for pore resistance (R_{pore}), and the coating capacitance (C_{coat}) plotted versus exposure time. The double layer capacitance and polarization resistance results are not presented as the indication of their presence within the data was not sufficient to allow the model to accurately predict their values.

Evaluation of the Figures 5 – 9 suggests the following sequential behavior:

- Penetration of the stripper into the coating began immediately, indicated by the C_{coat} parameter beginning to increase at a slowly accelerating rate (as the coating gains mass through penetrant diffusion, its charge storage capacity increases resulting in a larger capacitance).
- At approximately 5 hours 20 minutes, the impedance at 0.1 Hz ($Z_{f=0.1Hz}$) and the pore resistance (R_{pore}) began to decrease more rapidly, while the C_{coat} parameter continued to increase at a slowly accelerating rate. This indicated that the rate of stripper penetration into the coating as a function of mass was relatively unchanged, but the penetration rate, as a fraction of coating thickness, had increased. This could only result if the stripper was being drawn into the coating by a capillary mechanism along the sides of the pores, creating a deeper electrical conduction path into the coating and therefore a shorter resistive path through the coating than would result if the pores were sequentially filling. These results further indicate that the penetration of the stripper may have been restricted by a "skin layer" at the coating surface.
- At approximately 11 hours 20 minutes, the increase of the C_{coat} parameter slows, leveling off at approximately $1x10^{-8}$ F/cm^2. This indicates that the pore filling of the coating by the SARA stripper was complete and the stripper had reached the substrate.
- At approximately 13 hours 30 minutes, the rate of decrease of the $Z_{f=0.1Hz}$ and R_{pore} slows indicating that the coating had fully swelled.
- At 17 hours, the C_{coat} parameter increased abruptly indicating that stripping of the coating was complete.

Epoxy Polyamide Coating with Aluminum Pigment

The impedance and phase angle results for the epoxy polyamide coating with aluminum pigment at several stages throughout the stripping process are presented in Figures 10 and 11. These graphs again show noticeable trends in the impedance and phase angle behavior as a function time, illustrating the increasing effect of the SARA stripper on the coating as the stripping process proceeds.

Figures 12 through 14 show the values of the $Z_{f=0.1Hz}$ and the fitted circuit model elements R_{pore} and C_{coat} plotted versus exposure time. Again, the double layer capacitance and polarization resistance results are not presented as the indication of their presence within the data was not sufficient to allow the model to accurately predict their values.

.

Evaluation of the Figures 10 – 14 suggests the following sequential behavior:

- Penetration of the stripper into the coating began immediately, indicated by the C_{coat} parameter beginning to increase at a slowly accelerating rate.
- At approximately 6 hours, the $Z_{f=0.1Hz}$ and R_{pore} values began to decrease more rapidly, while the C_{coat} parameter continued to increase at a slowly accelerating rate. This again

indicated that the rate of stripper penetration into the coating was unchanged, but the penetration rate as a fraction of coating thickness had increased. Again, these results indicate that the penetration of the stripper was restricted by a "skin layer" at the coating surface, and that the further penetration of the stripper into the coating was dominated by a pore surface capillary mechanism rather than a volume filling mechanism.

- At approximately 9 hours 30 minutes, the rate of increase of the C_{coat} parameter stabilized indicating that the SARA stripper had reached the substrate.
- At 12 hours, the C_{coat} parameter abruptly increased indicating that stripping of the coating was complete.

Alkyd Coating with Titanium Dioxide Pigment

Figures 15 and 16 show the impedance and phase angle results for the alkyd coating system (all 3 coats with titanium dioxide pigment) at several stages throughout the stripping process. As with the epoxy coatings, these figures revealed the progressive effect of the SARA chemical stripper.

Figures 17 through 20 show the values of the $Z_{f=0.1Hz}$ and the fitted circuit model elements R_{pore}, C_{coat} and the double layer capacitance (C_{DL}) plotted against exposure time. The polarization resistance results are not presented as the indication of their presence within the data was not sufficient to reliably predict its value.

The action of the SARA chemical stripper can be characterized as follows:

- Penetration of the stripper into the coating began immediately, indicated by the C_{coat} parameter beginning to increase at a slowly accelerating rate.
- At approximately 15 minutes, the $Z_{f=0.1Hz}$ and R_{pore} values began to decrease more rapidly, while the C_{coat} parameter continued to increase art a slowly accelerating rate. This indicated that the rate of stripper penetration into the coating was unchanged, but the penetration rate as a fraction of coating thickness had increased. These results further indicate that the absorption of the stripper was restricted by a "skin layer" at the coating surface, and that the further penetration of the stripper into the coating is dominated by a capillary mechanism rather than a volume filling mechanism.
- At approximately 25 minutes the rate of decrease of the $Z_{f=0.1Hz}$ and R_{pore} values begins to slow indicating that pore filling is nearly complete.
- At approximately 35 minutes, the rate of increase of the C_{coat} parameter stabilized. This indicates that the pore filling of the coating by the SARA stripper was complete and the stripper had reached the substrate. This observation was reinforced by another rapid decrease in the $Z_{f=0.1Hz}$ and R_{pore} values.
- At approximately 50 minutes, the rate of decrease of the $Z_{f=0.1Hz}$ and R_{pore} values slowed and the C_{coat} abruptly increased indicating that stripping of the coating was complete. Also at 50 minutes, the value of C_{DL} can be determined from the data.

Alkyd Coating with Aluminum Flake (Leafing) Pigment

Figures 21 and 22 show the impedance and phase angle results for the alkyd coating system (mid and finish coats with leafing aluminum pigment) at several stages throughout the stripping process.

Figures 23 through 26 show the values of the $Z_{f=0.1Hz}$ and the fitted circuit model elements R_{PR}, C_{coat} and C_{DL} plotted versus exposure time. The polarization resistance results are not presented as the indication of their presence within the data was not sufficient to allow the model to accurately predict its value.

Evaluation of the Figures 21 – 26 suggests the following behavior:

- Penetration of the stripper into the coating began immediately, indicated by the C_{coat} parameter beginning to increase at a slowly accelerating rate.
- At approximately 30 minutes, the $Z_{f=0.1Hz}$ and R_{pore} values began to decrease more rapidly, while the C_{coat} parameter continued to increase at a slowly accelerating rate. This indicated that the rate of stripper absorption by the coating was relatively unchanged, but the penetration rate as a fraction of coating thickness had increased. These results further indicate that the absorption of the stripper was restricted by a "skin layer" at the coating surface, and that the further penetration of the stripper into the coating is dominated by a capillary mechanism rather than a volume filling mechanism.
- At 45 minutes it became possible to calculate the C_{DL} value indicating that the stripper had reached the substrate.
- At approximately 55 minutes the rate of decrease of the $Z_{f=0.1Hz}$ and R_{pore} values slowed. Also at 55 minutes, the rate of increase of the C_{coat} parameter slowed. These changes indicated that the pore filling of the coating by the SARA stripper was nearly complete.
- At approximately 1 hour 15 minutes the $Z_{f=0.1Hz}$ and R_{pore} values began to decrease more rapidly again. This also corresponded with the C_{coat} value stabilizing briefly at a near constant value. This indicated the onset of the coating being stripped from the substrate.
- At 1 hour 45 minutes, the $Z_{f=0.1Hz}$ and R_{pore} values stabilized at low values and the C_{coat} value increased abruptly indicating that stripping of the coating was complete.

Effect of TiO_2 pigment versus non-leafing aluminum pigment in epoxy polyamide coating

From the analysis of the EIS data, a comparison of the effect of the different pigments can be summarized in the following table.

	TiO_2 pigment	**Deleafed Aluminum pigment**
Stage of stripping	**Time from application of stripper**	
Penetration past "skin layer"	5 hr 20 min	6 hr 0 min
Pore filling complete	11 hr 20 min	9 hr 30 min
Stripping complete	17 hr 0 min	12 hr 0 min
Stage of stripping	D **Time**	
Pore Filling	6 hr 0 min	3 hr 30 min
De-adhesion	5 hr 40 min	2 hr 30 min

From the table it can be seen that although the aluminum particulate pigment resulted in a slower penetration of the SARA stripper past the "skin layer" (as compared to the TiO_2 pigment) the subsequent pore filling and final stripping occurred at approximately twice the rate.

The differential response of the aluminum pigmented epoxy and its titanium dioxide counterpart to stripping with the SARA stripper might well relate to the fact that the action of the stripper is catalyzed by contact with intra-film metal. This decomposes a component in the stripper to produce gaseous oxygen (adding porosity to the film). This exacerbates penetration, and deadhesion from the metal. Thus it can be expected that as the stripper penetrates into the epoxy containing the "stripped or deleafed" aluminum (i.e. the aluminum devoid of its fatty acid surface treatment) direct metallic contact and, therefore, catalysis and oxygen production within the film is possible.

The increased porosity would lead to the establishment of an interconnected pore network within the film, allowing more rapid penetration of the SARA material to the surface. Furthermore, this behavior would also increase the swelling experienced by the coating, arguably increasing the negative pressure at the coating-substrate interface, and arguably increasing the drive to disbond the coating from the substrate. Such metallic catalysis in the titanium dioxide pigmented film does not occur until the penetrant has reached the surface. Without intra-film metallic catalysis, the effectiveness of the SARA stripper relies on its penetration properties alone (at least until the stripper reaches the metallic substrate). Catalytic exacerbation of penetration does not, of course, occur in the penetration by water and/or ionic solutions.

Effect of TiO_2 pigment versus leafed aluminum pigment in the alkyd coating.

From the analysis of the EIS data, a comparison of the effect of the different pigments can be summarized in the following table.

	TiO_2 pigment	**Leafed Aluminum pigment**
Stage of stripping	**Time from application of stripper**	
Penetration past “skin layer”	15 min	30 min
Pore filling complete	35 min	1 hr 15 min
Stripping complete	50 min	1 hr 45 min
Stage of stripping	D **Time**	
Pore Filling	20 min	45 min
De-adhesion	15 min	30 min

While at first glance these results seem to be contradictory, they may be explained by examining the different behaviors exhibited by titanium dioxide and by leafing aluminum protected (at least to some extent) with low energy fatty acid treatments. As in the case of the epoxy there is no catalysis occurring in the body of the titanium dioxide pigmented alkyd film. That penetration is faster in the TiO_2 alkyd versus the epoxy is solely related to the much greater vulnerability of the binder matrix to penetration.

The alkyd film containing the leafing aluminum pigment is, however, less hospitable to ingress of the SARA stripper than is the titanium dioxide pigmented alkyd. This is because a greater percentage of the aluminum is segregated at the surface of the coating, where it packs into a quasi-metallic layer (Figure 27). As may be noted in the photomicrographs (Figure 28 and 29) the leafing properties of the aluminum in the alkyd (used in these experiments) are impeded, and the aluminum flakes are at least in part distributed throughout the film cross-section. However, this SARA penetration is much slower as the pathways around the particles are narrower and more tortuous). Where the leafing aluminum is itself protected with a still intact surface treatment, which insulates the aluminum from the stripper, the onset of catalysis will be slower. In a fully

leafed system the aluminum is present as a very high pigment volume content layer only in the upper layers of the film, and the oxygen tends to release directly from the film (at least, at first) without producing undue porosity in the binder. Below the aluminum layer there is a relatively low PVC layer of alkyd resin, until the aluminum layer of the intermediate and prime coat layers are reached. Penetration through this relatively lowly pigmented layer will be of the same order as that of the titanium dioxide film. In the present case, the alkyd aluminum film (here tested) is somewhat more homogeneous than is the fully leafed system, even if it is less homogeneous than the epoxy.

Thus the EIS results for the epoxy polyamide versus the alkyd coatings show that the epoxy polyamide possesses a substantially greater resistance to the SARA stripper. This is exhibited both in the rate of penetration of the stripper into the coating, which indicates a greater resistance to swelling and pore path creation, as well as in the rate of stripping, which indicates a higher bonding strength to the substrate.

A cross-sectional SEM of the leafing aluminum based alkyd film is, to reiterate, shown in Figures 28 and 29. It is clear that, while there is some slight heterogeneous accumulation of the aluminum flake in the surface layers of the film, the majority of the flake is homogeneously distributed throughout the film thickness. Thus leafing is greatly diminished from what it might be, and the rate of stripper movement through the film more closely mirrors movement through the epoxy than it might have been were the alkyd film to have been fully leafed.

Figure 30 is an optical micrograph of the chemically stripped alkyd that contained titanium dioxide. Close inspection reveals the shrivelled structure of the alkyd after it had been penetrated by the SARA chemical stripper.

Conclusions

The EIS technique utilizing a novel and customized cell has produced quantitative measurements that provide insights into the internal changes in a coating's barrier property behavior during chemical stripping.

Results from EIS investigations correlated well with the expected coating behaviors based on the coating pigment chemistry and structure, as well as the chemical composition of the binder resins employed.

The EIS evaluations were able to detect (a) the penetration of the stripper into alkyd and epoxy coatings, (b) the arrival of the stripper at the coating-substrate interface, and (c) the removal of the coating from the substrate.

EIS gave important insights into the behavior of the SARA chemical stripper as it interacted with different generic coating types and their different pigments.

REFERENCES

1. O'Donoghue M, Garrett R, Graham R, Datta V.J., Vitomir S, White D, and Peer L, Chemical Strippers and Surface-Tolerant Coatings: A Tandem Approach for Steel and Concrete". JPCL Vol. 17, p.74-93, May 2000.

2. Hare .C.H, Effects of Solvents on Coating Films, JPCL, May 1997, p.69.

3. SSPC-TU6: Chemical Stripping of Organic Coatings from Steel Structures, SSPC Publication No.99-09, ISBN 1-889060-37-2.

4. Funke W, Towards Environmentally Acceptable Corrosion Protection by Organic Coatings. Problems and Realization. Journal of Coatings Technology vo.55, No.705, October. 1983.

5. Hare C.H, Aluminum Pigments Rate Best in Barrier Systems Study. Modern Plant and Coatings, December 1985.

6. O'Donoghue M, Garrett R, Datta V.J, Meli P. Jr., Meilus L. Optimizing Performance of Fast-Cure Epoxies for Pipe and Tank Linings: Chemistry, Selection, and Application, JPCL, March 1998, p.36.

7. Bacon R.C, Smith J.J, and Rugg F.M, "Electrolytic Resistance in Evaluating the Protective Merit of Coatings on Metal" Ind. Eng. Chem. 1948, 40, 161.

8. Leidheiser H. Jr., Towards a Better Understanding of Corrosion Beneath Organic Coatings. Corrosion, May 1983, 190.

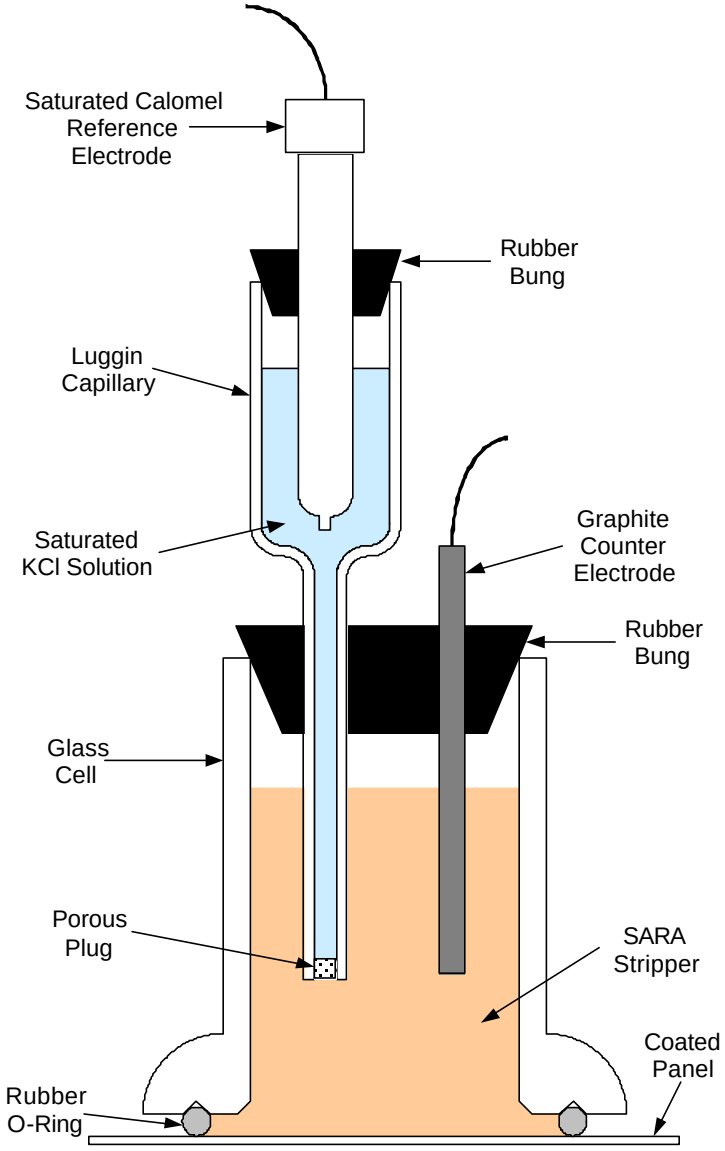

Figure 1: EIS Test Apparatus

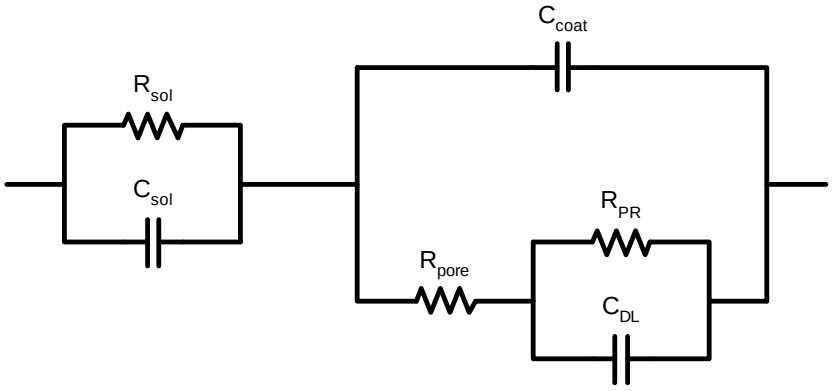

R_{sol} = Solution Resistance

R_{pore} = Pore Resistance

C_{sol} = Solution Capacitance

R_{PR} = Polarization Resistance

C_{coat} = Coating Capacitance

C_{DL} = Double Layer Capacitance

Figure 2: Equivalent Circuit Model for EIS Data Evaluation

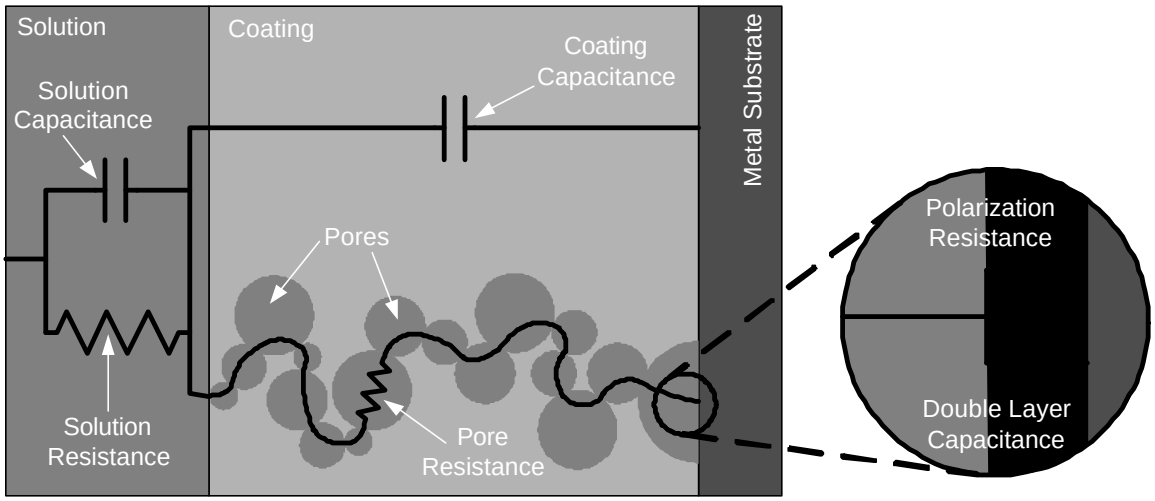

Figure 3: Relationship between circuit model and physical coating and corrosion properties. (Solid lines indicate possible current paths.)

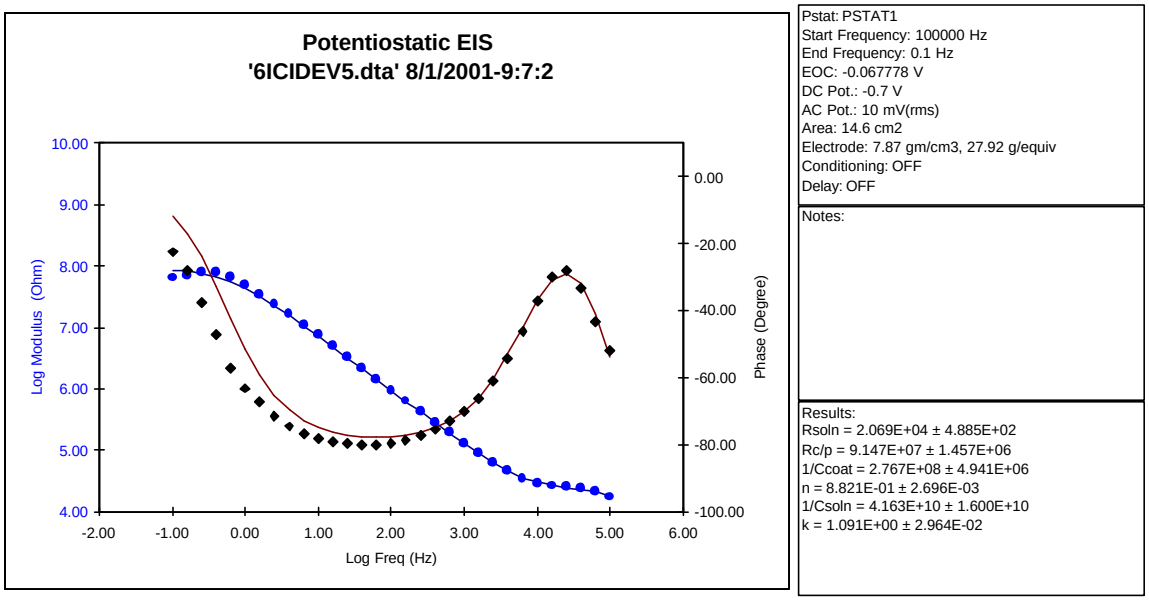

Figure 4: Example of the circuit model fit to an EIS scan from the present study. (dots are impedance data points, diamonds are phase angle data points, and solid lines are the circuit model fit curves.)

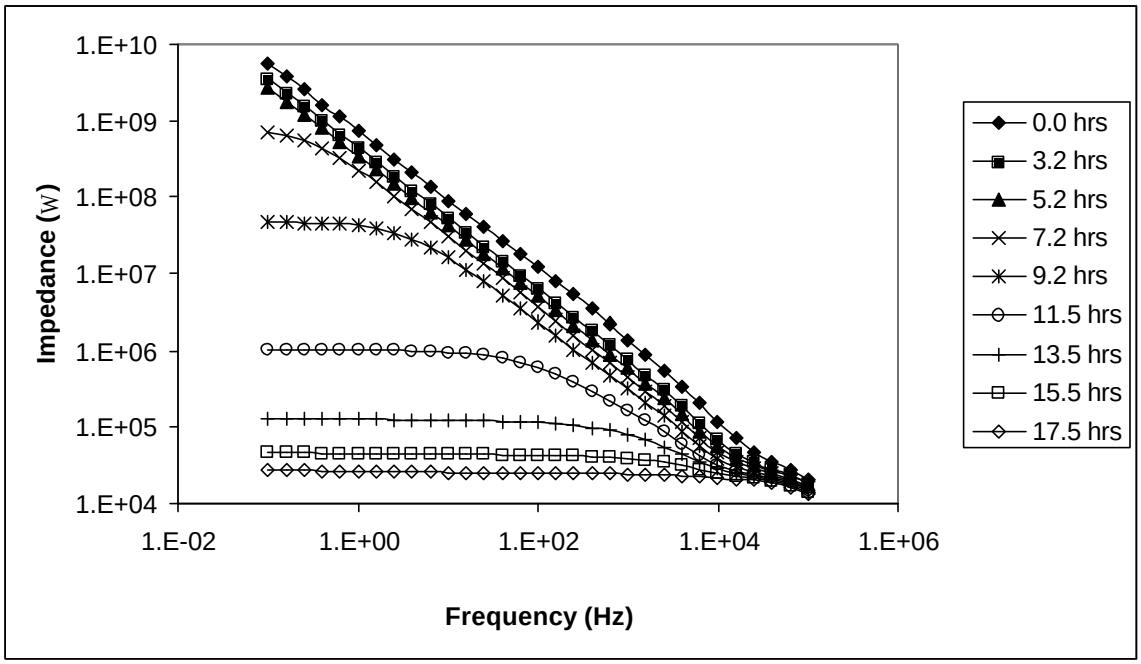

Figure 5: Impedance results for epoxy coating with TiO_2 pigment

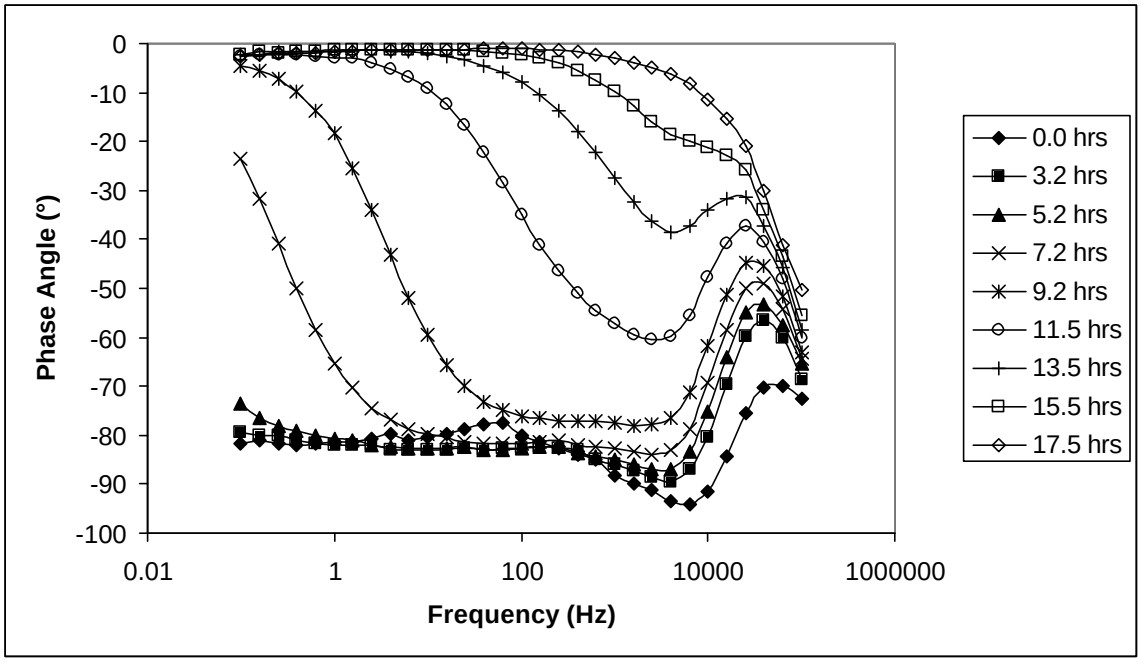

Figure 6: Phase angle results for epoxy coating with TiO_2 pigment

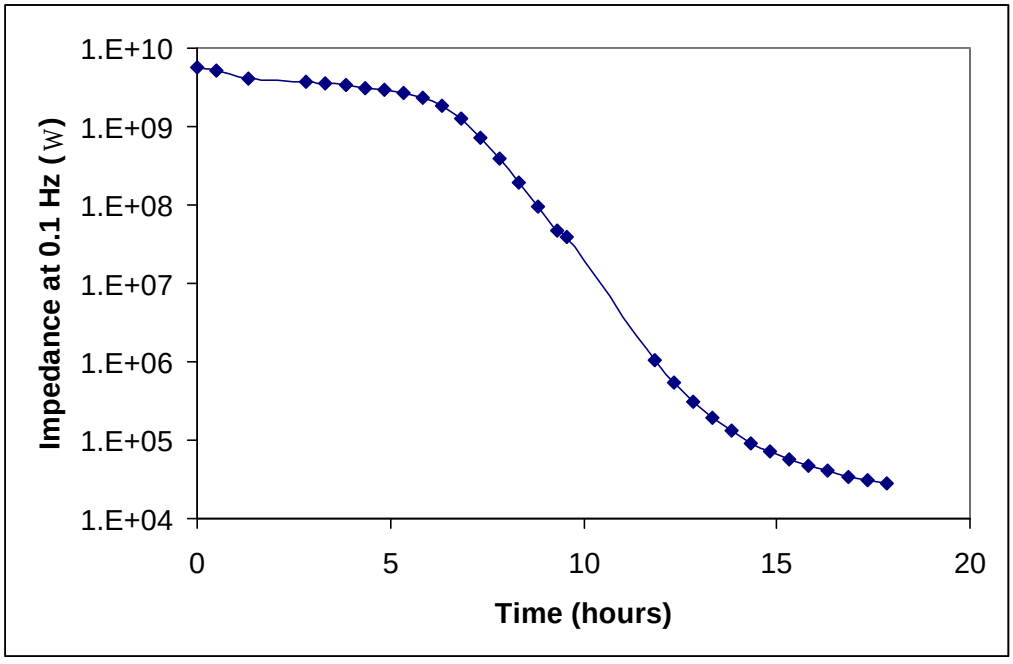

Figure 7: Impedance at 0.1Hz vs. time for epoxy coating with TiO_2 pigment

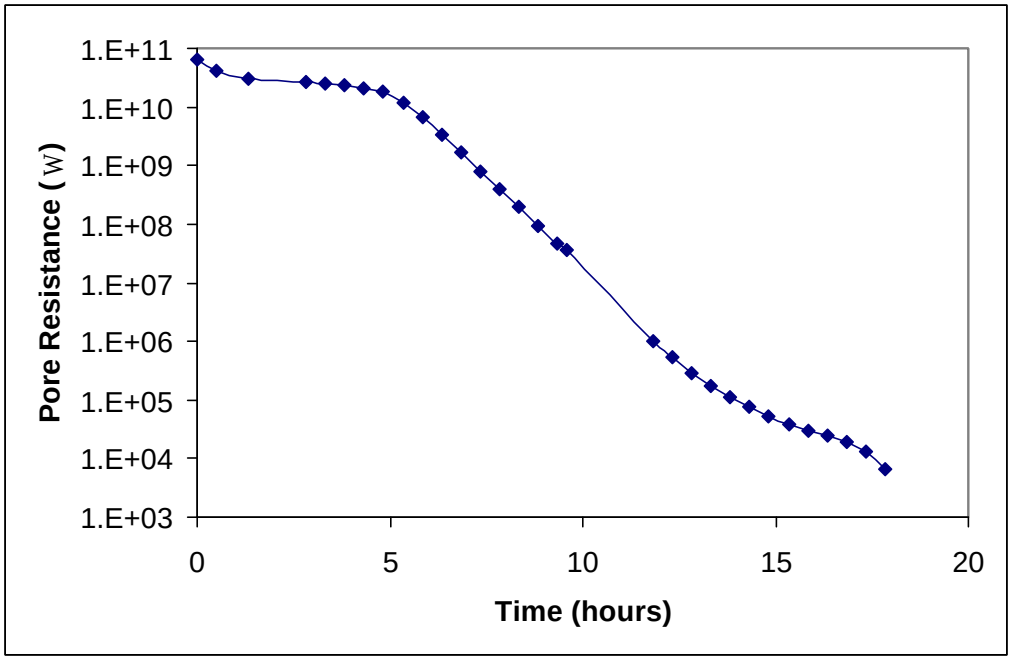

Figure 8: Pore resistance vs. time for epoxy coating with TiO_2 pigment

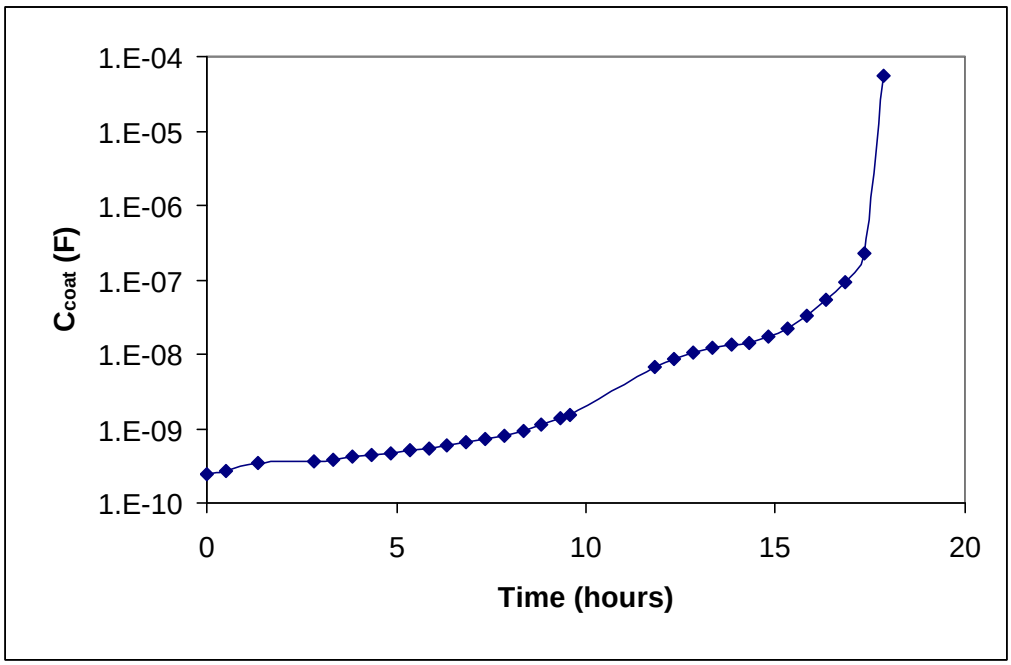

Figure 9: Coating Capacitance vs. time for epoxy coating with TiO_2 pigment

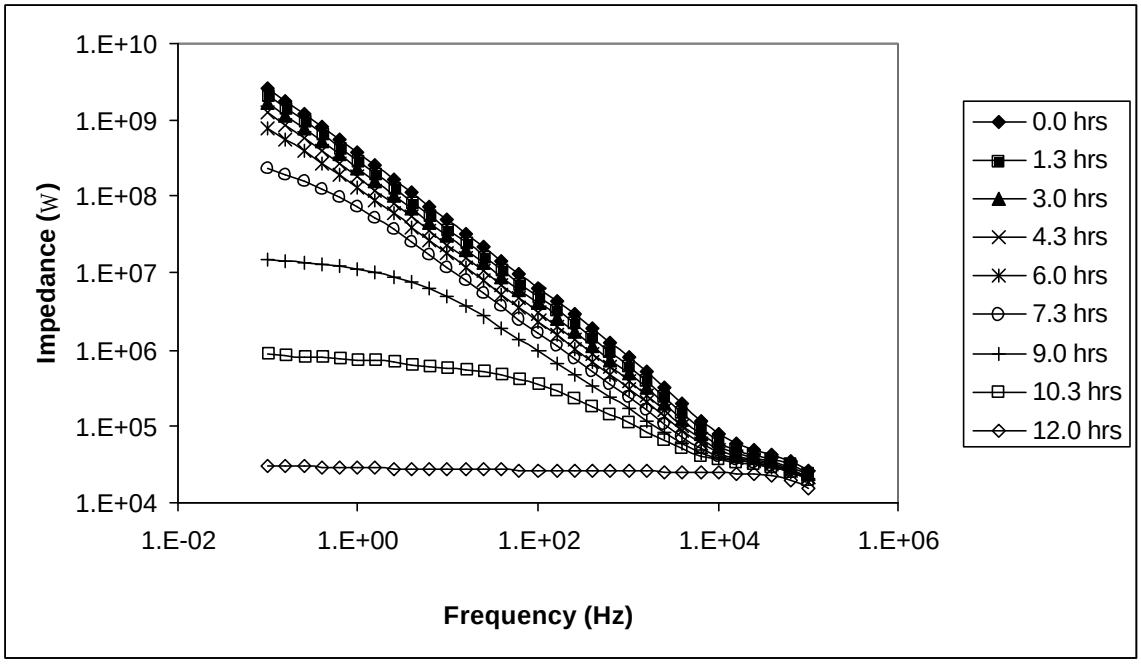

Figure 10: Impedance results for epoxy coating with de-leafed aluminum pigment

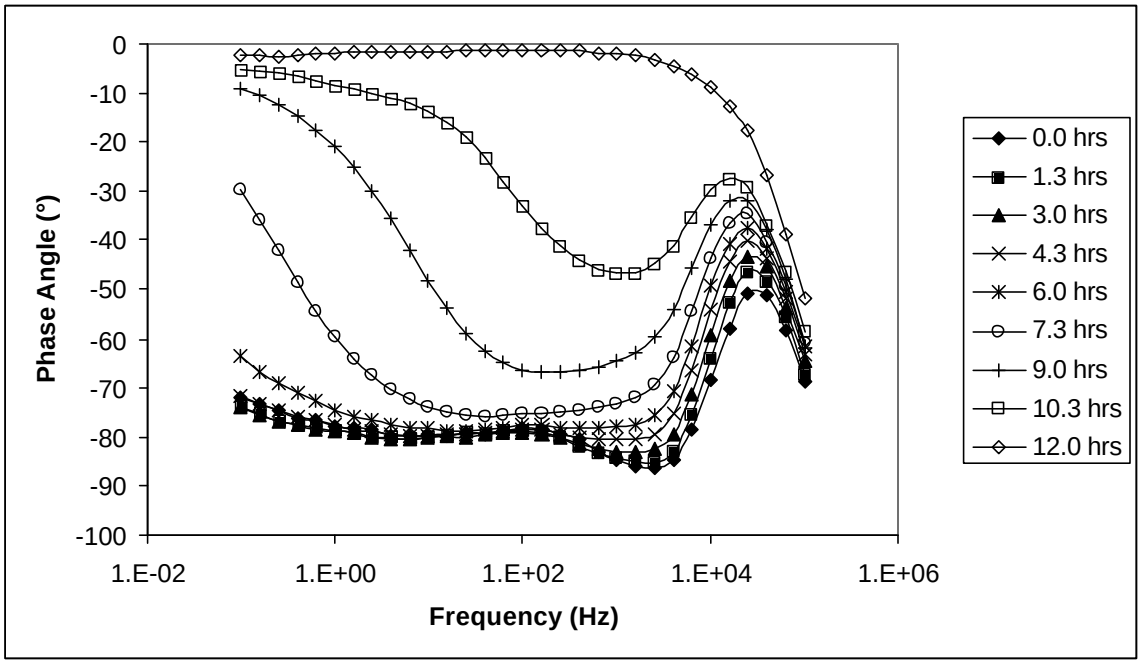

Figure 11: Phase angle results for epoxy coating with de-leafed aluminum pigment

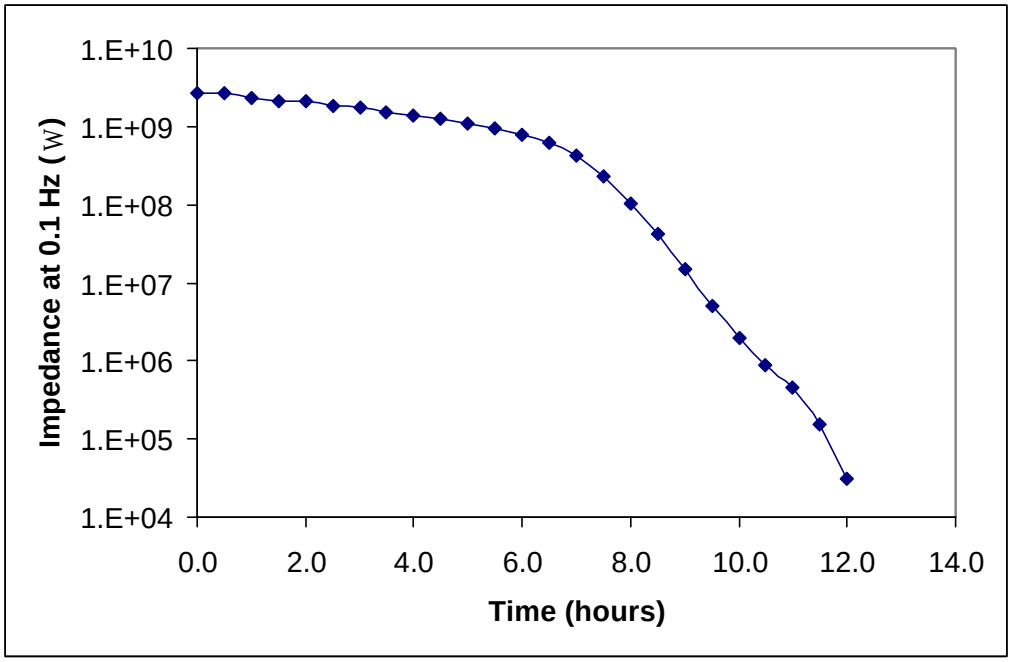

Figure 12: Impedance at 0.1Hz vs. time for epoxy coating with de-leafed aluminum pigment

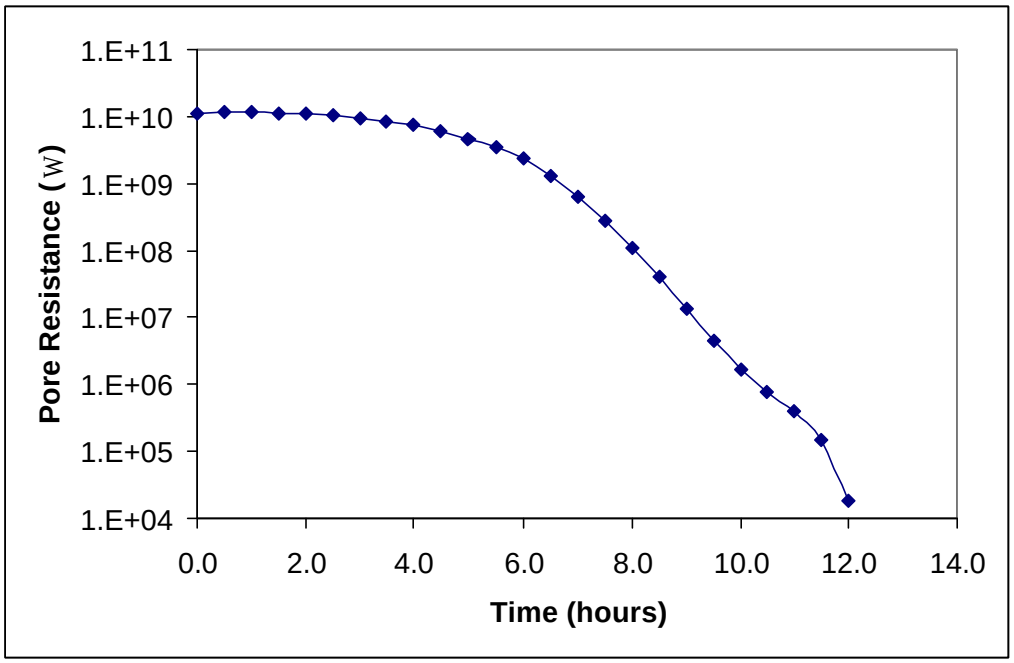

Figure 13: Pore resistance vs. time for epoxy coating with de-leafed aluminum pigment

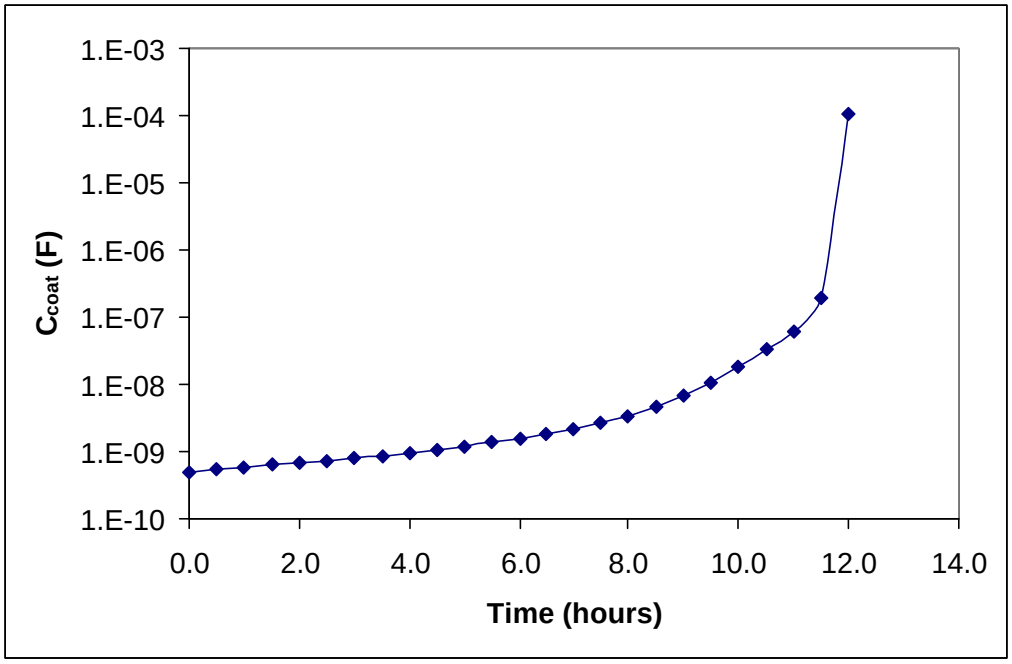

Figure 14: Coating Capacitance vs. time for epoxy coating with de-leafed aluminum pigment

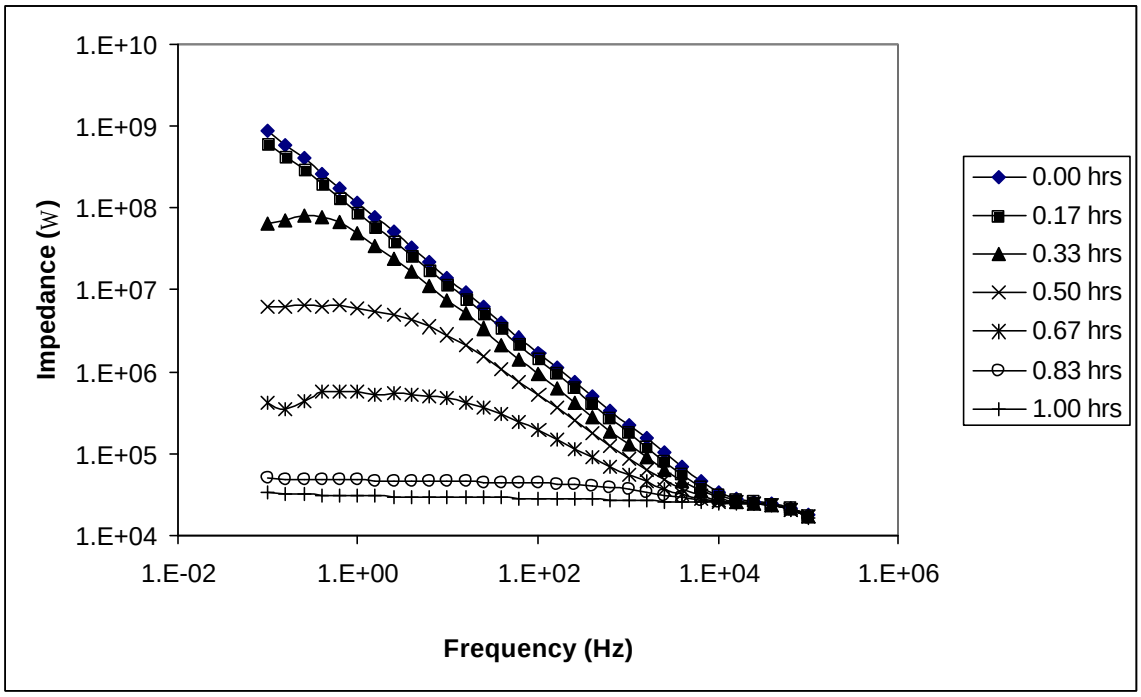

Figure 15: Impedance results for alkyd coating with TiO_2 pigment

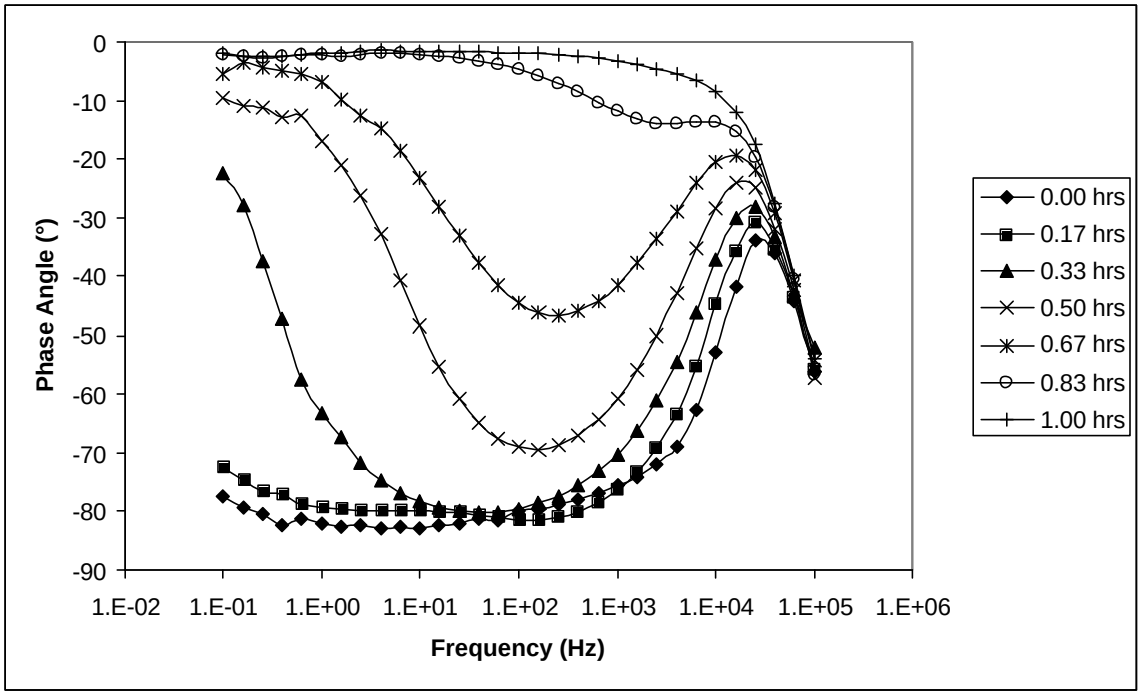

Figure 16: Phase angle results for alkyd coating with TiO_2 pigment

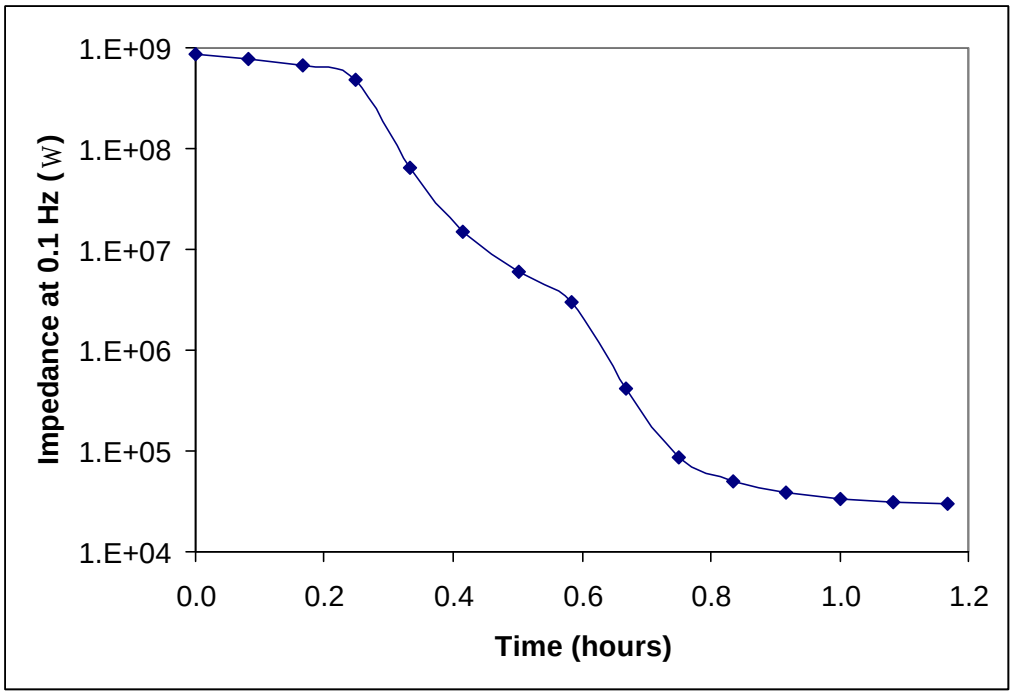

Figure 17: Impedance at 0.1Hz vs. time for alkyd coating with TiO_2 pigment

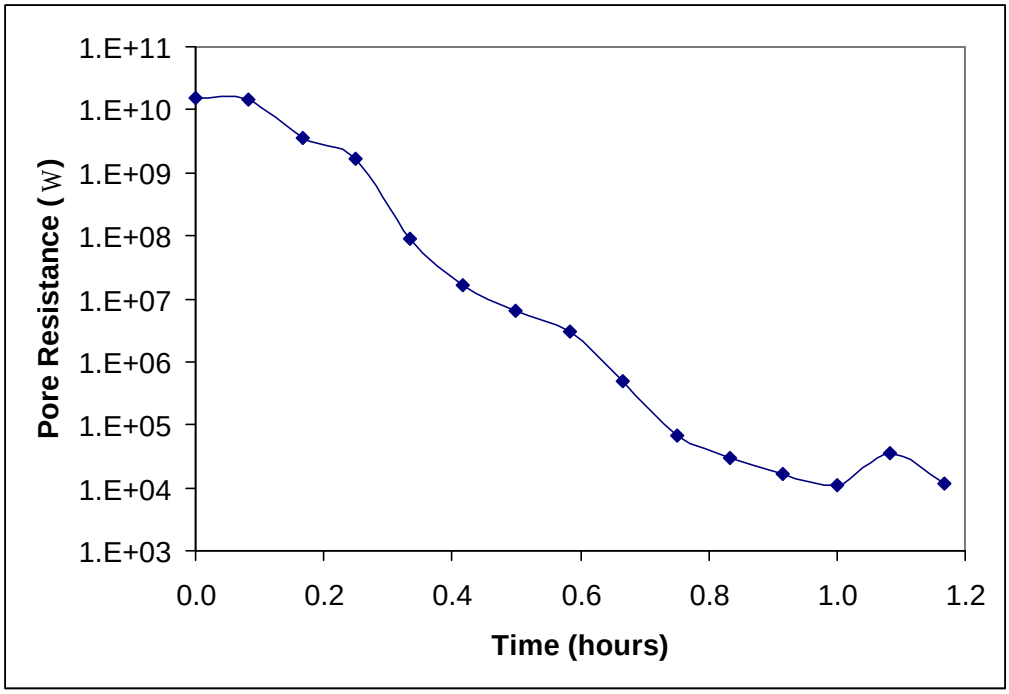

Figure 18: Pore resistance vs. time for alkyd coating with TiO_2 pigment

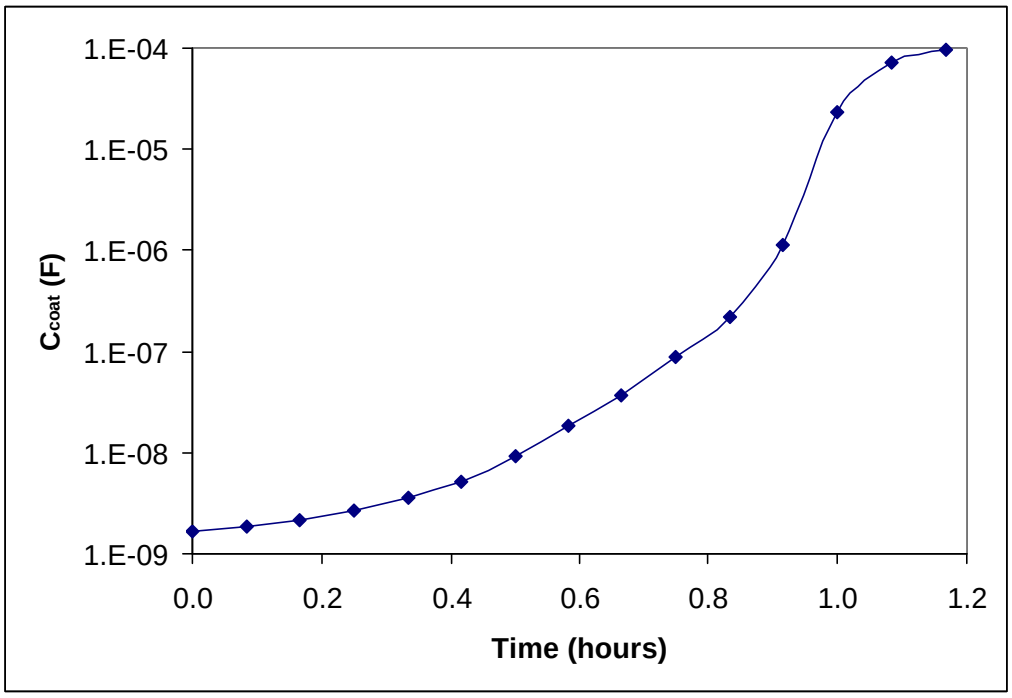

Figure 19: Coating Capacitance vs. time for alkyd coating with TiO_2 pigment

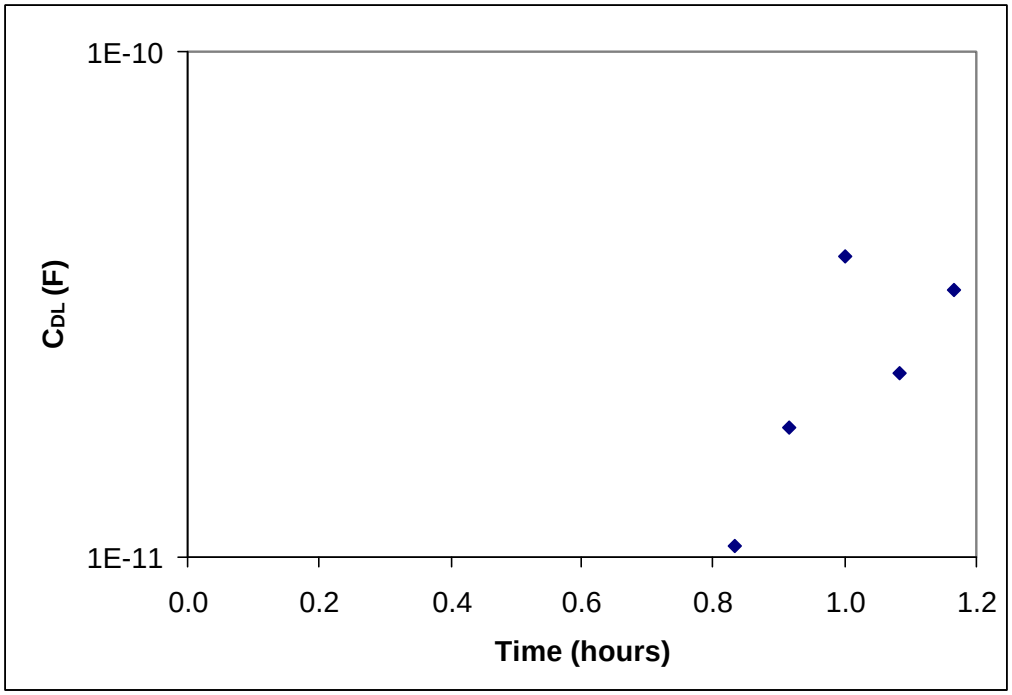

Figure 20: Double Layer Capacitance vs. time for alkyd coating with TiO_2 pigment

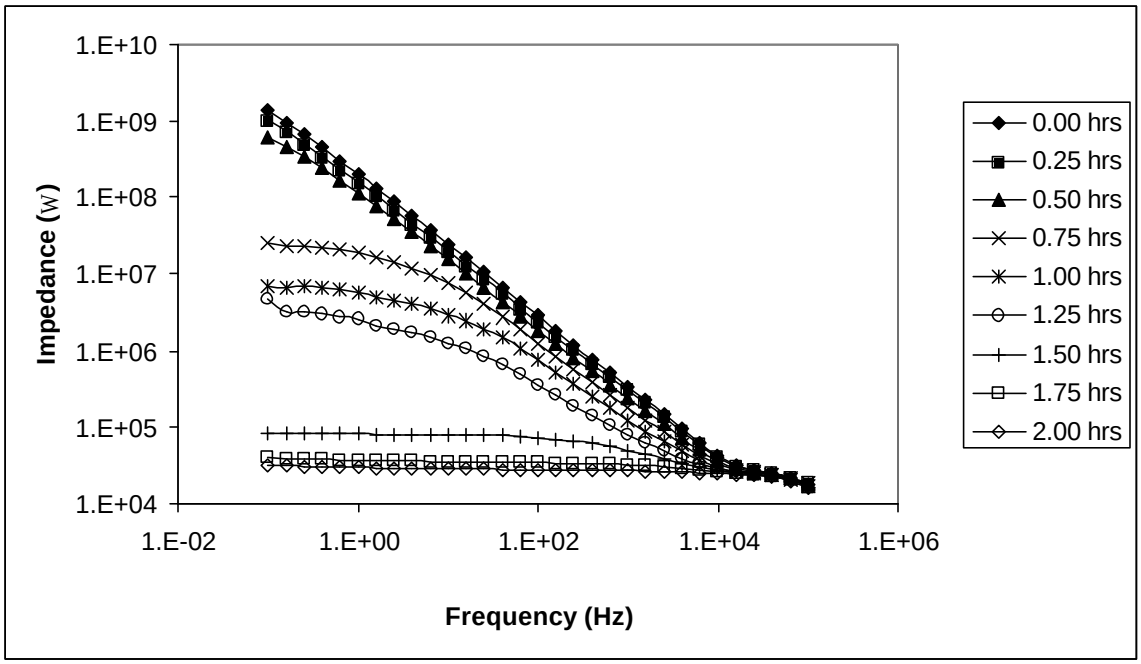

Figure 21: Impedance results for alkyd coating with leafing aluminum pigment

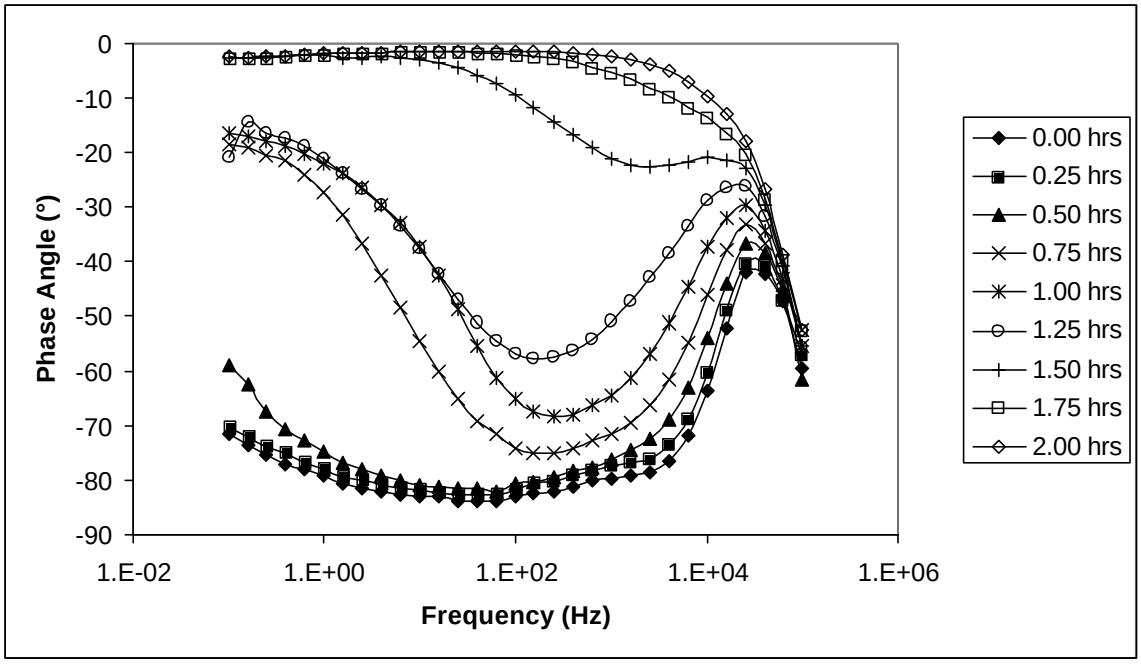

Figure 22: Phase angle results for alkyd coating with leafing aluminum pigment

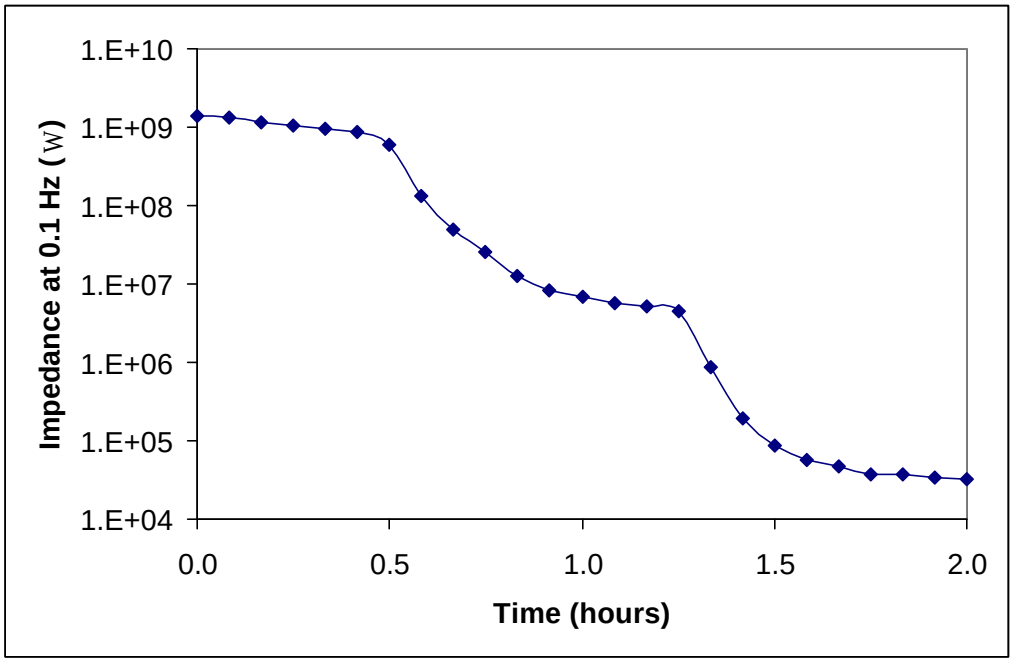

Figure 23: Impedance at 0.1Hz vs. time for alkyd coating with leafing aluminum pigment

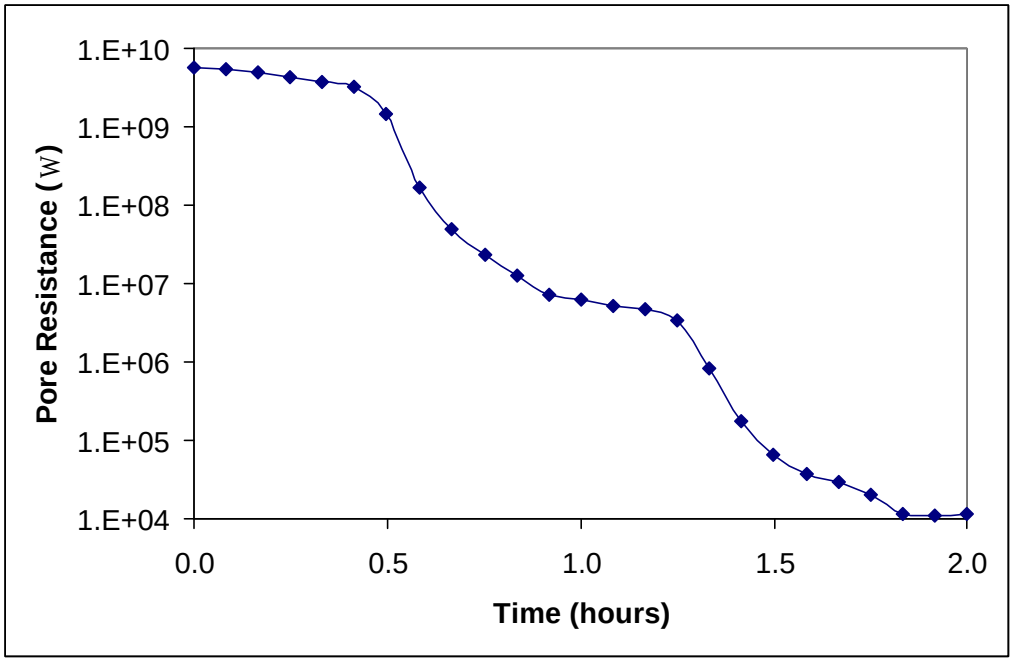

Figure 24: Pore resistance vs. time for alkyd coating with leafing aluminum pigment

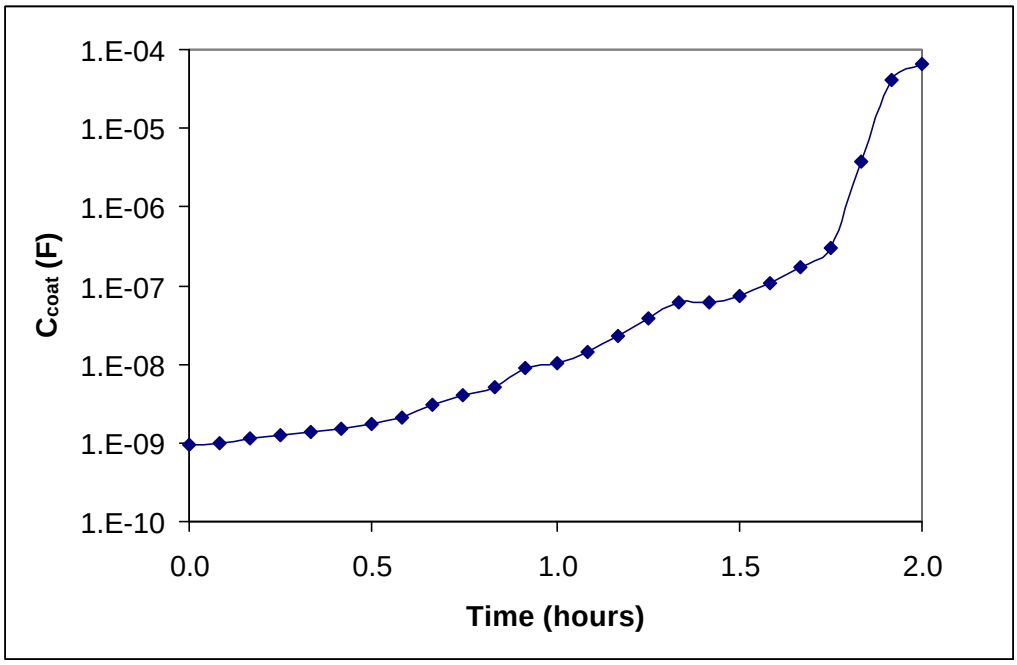

Figure 25: Coating Capacitance vs. time for alkyd coating with leafing aluminum pigment

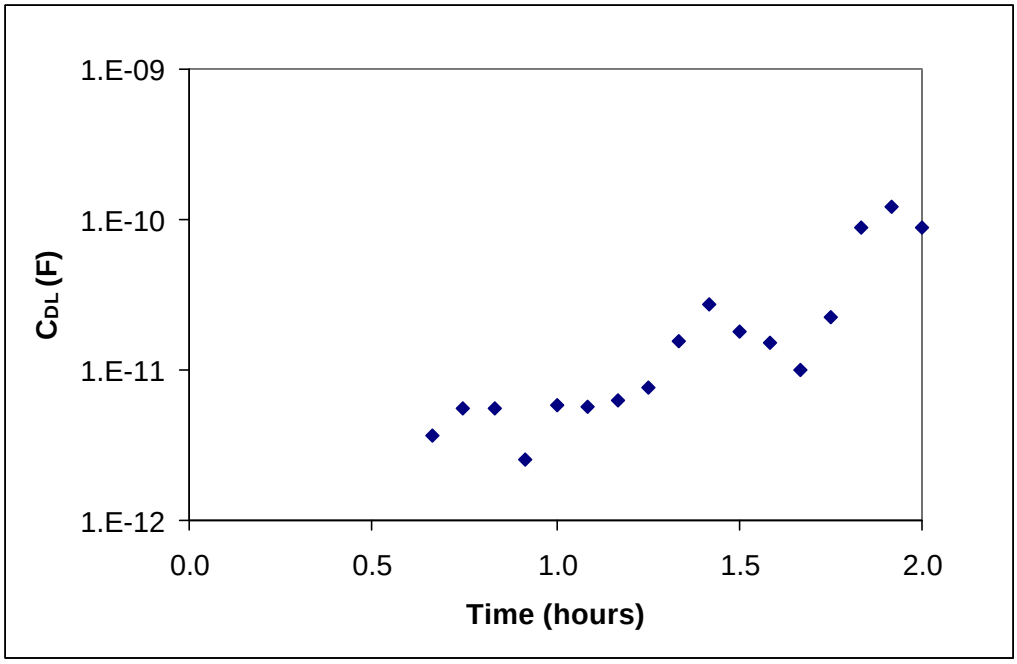

Figure 26: Double Layer Capacitance vs. time for alkyd coating with leafing aluminum pigment

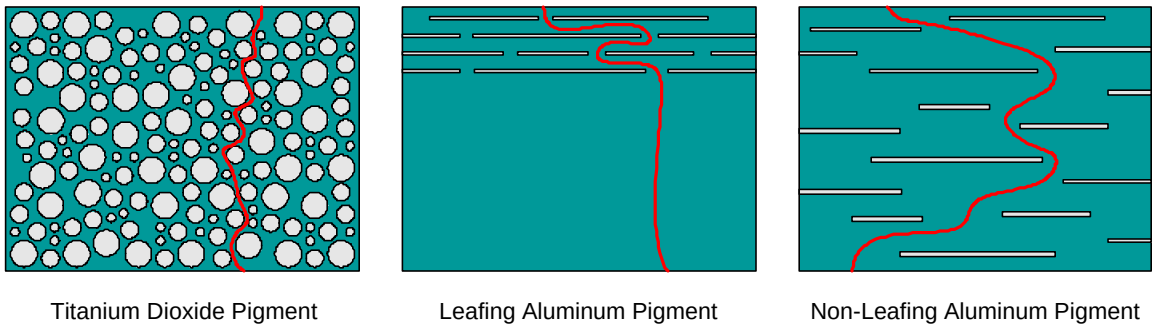

Figure 27: Coating structures containing titanium dioxide pigment versus leafing aluminum flake and non-leafing aluminum flake pigments.

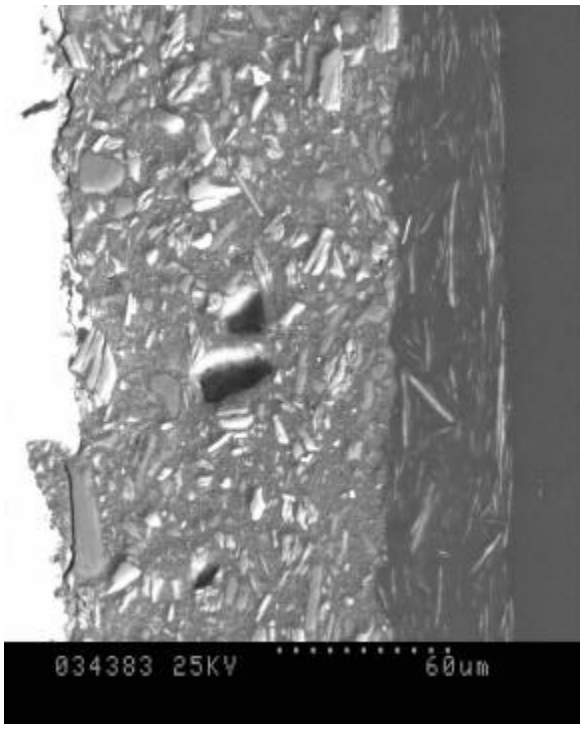

Figure 28: Electron Micrograph of the Alkyd finish containing leafing aluminum paste that had de-leafed

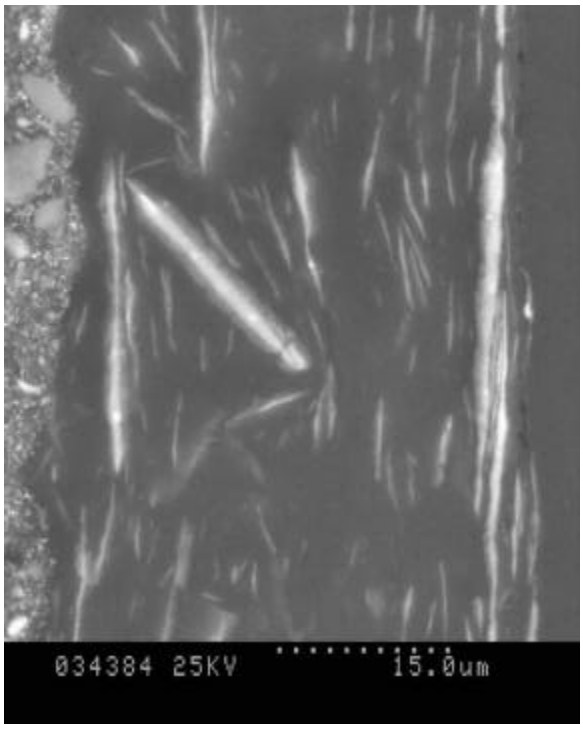

Figure 29: Close-up of de-leafed aluminum pigment shown in Figure 29

Figure 30: Optical micrograph of the chemically stripped alkyd finish containing TiO2 and the interface with bare steel. Note the shriveled appearance of the stripped alkyd finish.